Quaternary Science Reviews 192 (2018) 97–105

Contents lists available at ScienceDirect

Quaternary Science Reviews

journal homepage: www.elsevier.com/locate/quascirev

Holocene temperature and hydrological changes reconstructed by bacterial 3-hydroxy fatty acids in a stalagmite from central China

Canfa Wang [a, b], James A. Bendle [b], Hongbin Zhang [a], Yi Yang [a], Deng Liu [a], Junhua Huang [c], Jingwei Cui [d], Shucheng Xie [a, *]

[a] State Key Laboratory of Biogeology and Environmental Geology, School of Earth Sciences, China University of Geosciences, Wuhan, 430074, China
[b] School of Geography, Earth and Environmental Sciences, University of Birmingham, Birmingham, B15 2TT, UK
[c] State Key Laboratory of Geological Processes and Mineral Resources, China University of Geosciences, Wuhan, 430074, China
[d] Research Institute of Petroleum Exploration and Development, PetroChina, Beijing 100083, China

ARTICLE INFO

Article history:
Received 26 October 2017
Received in revised form
13 April 2018
Accepted 21 May 2018

Keywords:
Holocene
Paleoclimatology
Novel proxy
3-Hydroxy fatty acid
China
Monsoon
Speleothems

ABSTRACT

To achieve a sufficient understanding of the spatial dynamics of terrestrial climate variability, new proxies and networks of data that cover thousands of years and run up to the present day are needed. Here we show the first Gram-negative bacterial 3-hydroxy fatty acid (3-OH-FA) based temperature and hydrological records from any paleoclimate archive globally. The data, covering the last 9 ka before present (BP), are generated from an individual stalagmite, collected from Heshang Cave, located on a tributary of the Yangtze River, central China (30°27′N, 110°25′E; 294 m). Our results indicate a clear early-to-middle Holocene Climatic Optimum (8.0–6.0 ka BP) followed by a long-term monotonic cooling and increasing variability over the last 0.9 ka BP. The hydrological record shows two relatively long wet periods (8.8–5.9 ka BP and 3.0–0 ka BP) and one relatively dry period (5.9–3.0 ka BP) in central China. We show that 3-OH-FA biomarkers hold promise as independent tools for paleoclimate reconstruction, with the potential to deconvolve temperature and hydrological signals from an individual stalagmite.

1. Introduction

Nearly half of the Earth's population live within the influence of the modern monsoon and its importance to terrestrial eco-systems, societal wellbeing and the global economy can not be overstated (Webster et al., 1998). Records of past Holocene rainfall and temperature, which extend the relatively short instrumental record, can constrain natural monsoon variability and are particularly important for the Asian monsoon region where prediction of future changes in rainfall using climate models has proven challenging (IPCC, 2014). Such records can also illustrate the influence of the monsoon on prehistoric cultures and settlements (Xie et al., 2013).

Stalagmites have become a key archive in Quaternary paleoclimatic reconstruction due to their ability to yield continuous and undisturbed records, precise and absolute chronologies, and their global terrestrial distribution (Blyth et al., 2016; Fairchild et al., 2006; Fairchild and Baker, 2012; McDermott, 2004; Wong and Breecker, 2015). Oxygen isotopes are effectively the 'master' or standard approach for speleothem analysis, but inherently encode a mix of climatic signals (Lachniet, 2009; McDermott, 2004), including, at the regional scale, temperature changes, the isotopic composition of source waters and precipitation amount. In addition, complex site-specific factors must be taken into account, such as drip rate (Dreybrodt and Scholz, 2011) and $CaCO_3$ precipitation (Fairchild and Baker, 2012). Many previous studies have focused on the interpretation of oxygen isotopes in speleothems, but deconvolving independent temperature and precipitation signals from speleothem $CaCO_3$ remains highly challenging, as evidenced by the paucity of such deconvolved records (Hu et al., 2008b; Yuan et al., 2004).

Biomarker based proxies are now firmly established in the fields of paleoceanography and paleolimnology (Castañeda and Schouten, 2011; Eglinton and Eglinton, 2008; Schouten et al., 2013). Recently attention has turned to the potential of organic matter and biomarker techniques for speleothem research (Blyth et al., 2008, 2016). A number of biomarkers with known paleoclimatic utility have been discovered and measured in speleothems, including glycerol dialkyl glycerol tetraethers (GDGTs) (Blyth et al.,

* Corresponding author.
E-mail address: xiecug@163.com (S. Xie).

https://doi.org/10.1016/j.quascirev.2018.05.030
0277-3791/

2014; Blyth and Schouten, 2013; Yang et al., 2011), plant derived biomarkers (Blyth et al., 2007, 2010, 2011; Bosle et al., 2014; Xie et al., 2003), branched fatty acids and hydroxy fatty acids (Blyth et al., 2006; Huang et al., 2008; Wang et al., 2012). Furthermore, Blyth and Schouten (2013) recently proposed a novel GDGT calibration, based on samples derived from 33 globally distributed speleothems from caves with a range of average air temperatures.

Biomarkers in stalagmites may originate from the overlying vegetation, overlying soil ecosystem, limestone aquifer and cave fauna (Blyth et al., 2008). Moreover, different biomarker classes may have different sources. For example, Yang et al. (2011) found that the majority of the archaeal isoprenoid and bacterial branched GDGTs measured in stalagmite samples from Heshang Cave were likely produced *in situ*. Most recently, Blyth et al. (2014) found that GDGTs preserved in stalagmites in the UK and Australia likely originated from the *in situ* microbial communities within cave systems. An artificial irrigation experiment conducted in Cathedral Cave, Australia, found different GDGT distributions among speleothem, soil and drip water samples (Baker et al., 2016). In contrast, a 2-year monitoring experiment of drip waters in Heshang Cave found that fatty acids in drip waters were most likely derived from the overlying soil and/or groundwater system via particulate entrainment and deposition (Li et al., 2011). It is noteworthy that the fatty acid ratios (ratios of $nC_{16:1}/nC_{16:0}$ and $nC_{18:1}/nC_{18:0}$; the prefix *n* indicates normal, the number before the colon specifies the number of C atoms, and the number after the colon gives the number of double bonds) showed a strong negative relationship with the external temperature recorded in Yichang meteoric station (located ca.100 km east of Heshang Cave), whereas the two ratios displayed no relationship with internal cave temperatures recorded at the HS4 site, which suggests that *in situ* cave microbes are probably not the predominant source for C_{16} and C_{18} acids in drip water collected in Heshang Cave. Li et al. (2011) concluded that, based on the distributional patterns of the fatty acids, microbes living in the overlying soils and/or groundwater system are the dominant source of fatty acids to the Heshang Cave drip waters. We note that Vaughan et al. (2011) discovered microbes living on speleothem surfaces in Kartchner Caverns, USA. Such consortia of microbes are an inevitable source of *in situ* fatty acids. Thus fatty acids measured in stalagmites may be derived from mixed sources, including overlying soils/sediments (Li et al., 2011), the ramifying network of conduits and reservoirs in the limestone and *in situ* microbes (Vaughan et al., 2011). However, even though the origin and pathways of inclusion into speleothems of biomarkers may be complex (Blyth et al., 2008, 2016), it doesn't hinder the utilization of biomarkers in paleaoclimate reconstruction. Site specific interpretation and ground truthing are required, but this is also true for established paleoclimate techniques, as outlined above. In summary, lipid biomarkers preserved in speleothems show clear potential for paleoclimate reconstruction. However, very few such biomarker based paleoclimatic reconstructions have been published (Blyth et al., 2011; Huguet et al., 2018; Li et al., 2014; Xie et al., 2003).

Gram-negative bacterial 3-hydroxy fatty acids (3-OH-FAs) are abundant in stalagmites (Blyth et al., 2006; Huang et al., 2008; Wang et al., 2012, 2016) and are characteristic compounds of Lipid A, the lipid component of the lipopolysaccharides (LPS) located in the outer membrane of Gram-negative bacteria (Szponar et al., 2002, 2003; Wollenweber and Rietschel, 1990). Based on the strong relationships with environmental pH and temperature from an altitudinal transect of soils on Shennongjia Mountain, central China, a number of novel 3-OH-FA based proxies have been proposed (Wang et al., 2016). For example, the ratio of *anteiso* to *normal* C_{15} 3-hydroxy fatty acid (RAN_{15}) was propounded to be a novel temperature proxy, and the ratio of the total sum of *iso* (*i*-) and *anteiso* (*a*-) 3-OH-FAs to the total amount of *normal* (*n*-) 3-OH-FAs (Branching Ratio) and the negative logarithm of Branching Ratio (RIAN) were propounded to be novel pH proxies (Wang et al., 2016).

In this study we present inferred temperature and hydrological records, spanning the last 9 ka BP, based on 3-OH-FA derived proxies from a single stalagmite collected from Heshang Cave, central China (Fig. 1). This work is the first demonstration of the application of 3-OH-FA based proxies for paleoclimatic reconstruction and suggests that such approaches may be used to derive independent quantitative temperature and qualitative hydrological signals from an individual stalagmite.

2. Materials and methods

2.1. Sampling site and sample information

Heshang Cave is located at 294 m above sea level (a.s.l.), on the Qing River, a tributary in the middle reaches of the Yangtze River, central China (30°27′N, 110°25′E) (Fig. 1A). Heshang Cave is one of several caves which characterize the regional karst landscape. The overlying dolomite is ca. 400 m thick and is capped with a mature layer of soil (20-40 cm-thick) and reasonably dense vegetation (Fig. 1B). The regional climate is strongly impacted by the East Asian Monsoon, with a hot and moist summer, but relatively cold and dry winter (An, 2000). Regional average annual precipitation is 1161 mm, based on the recent 64 years (1951–2014) of meteorological data from Yichang station. The seasonal temperature ranges, inside and immediately outside the cave, were constrained by 2-h resolution logging between 2004 and 2007 using HOBO H8 Pro T loggers (Hu et al., 2008a). The modern temperature immediately outside the cave varies seasonally from 3 °C to 30 °C, with an annual average of 18 °C and is statistically identical to that of the nearest government meteorological station in Changyang county (Hu et al., 2008a). The annual mean temperature inside the cave is identical to the outside measurements. However, the amplitude of the internal temperature range is about one fifth of the external cycle and lags the external temperatures by about 10 days (Hu et al., 2008a). Heshang Cave extends a distance of ≈250 m, roughly horizontally from it's entrance (see Fig. 1C) and is well decorated with stalagmites, rimstone pools, and less frequent stalactites (including an exquisite 'Lotus Flower' stalactite).

The HS4 stalagmite is 2.5 m long, and was actively growing when collected from ca. 150 m within Heshang Cave in 2001 (Fig. 1C). It shows clear annual banding throughout its growth axis, generated by the strong seasonal cycle at this site (Johnson et al., 2006). Highlights of previous work on this stalagmite include a quantitative Holocene Asian monsoon rainfall record (Hu et al., 2008b) and high resolution 8.2 ka event record (Liu et al., 2013; Owen et al., 2016). The HS4 stalagmite was divided longitudinally into 4 sections. Each section was dedicated to a different branch of analyses (e.g. $\delta^{18}O$, trace elements, organic geochemistry etc.). 206 subsamples were taken from the organic geochemistry section along the stalagmite growth axis and 73 subsamples were selected at intervals for biomarker analysis. All the outer layers of the subsample were removed during sampling to avoid any potential contamination. Based on annual layering each sample has a resolution of several decades to >100 years.

In 2013 seventeen cave sediment samples were collected within Heshang Cave from the entrance to the deepest accessible part of the cave (Fig. 1C) and nine overlying soil samples were collected from the land-surface immediately above the cave (which slopes upwards from an altitude of 457 m–489 m) (Fig. 1B). The sediment inside the cave is oligotrophic with <6 g/kg total organic carbon (Gong et al., 2015).

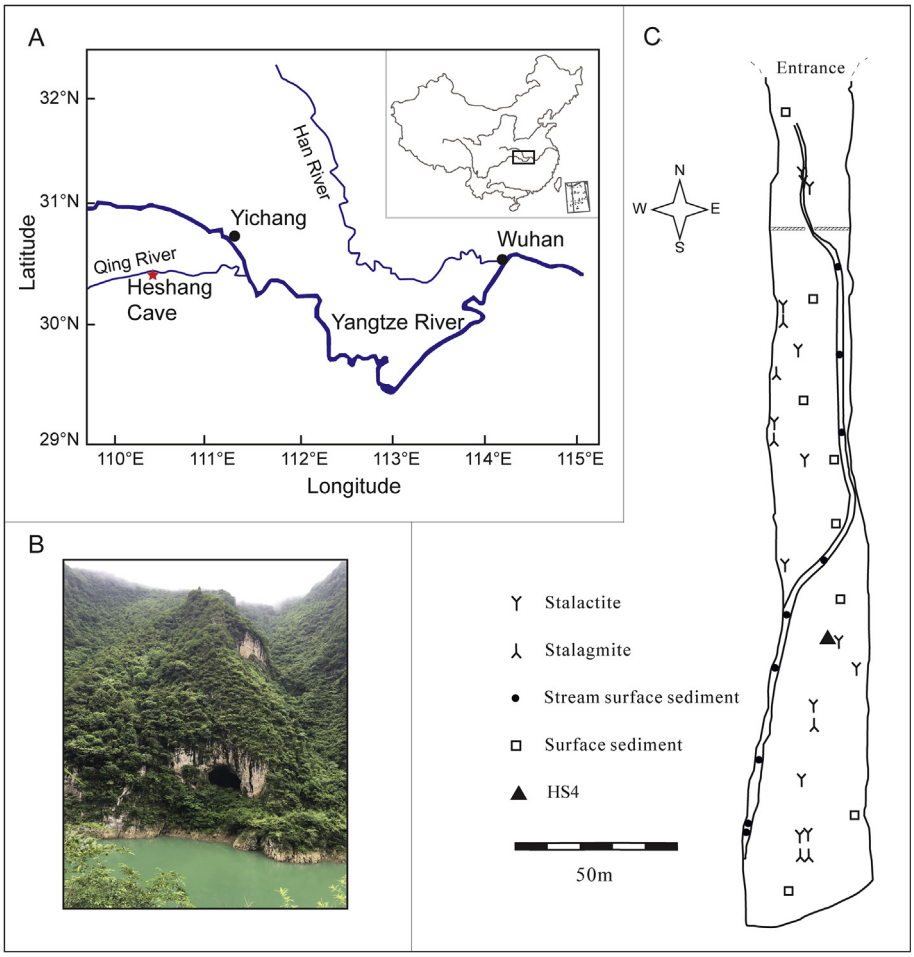

Fig. 1. The location of Heshang Cave and sample sites. A) Schematic map showing the main regional surface drainage, revised after Hu et al. (2008a). The red star shows the location of Heshang Cave. B) The view of Heshang Cave entrance from the opposite site of the Qing River. C) Sampling locations of HS4 stalagmite and cave surface sediments. Black solid triangle denotes the location of HS4 which was collected in 2001 (Hu et al., 2008a). Black solid circles denote the sampling sites of stream surface sediments; hollow squares denote the sampling sites of cave surface sediment. (For interpretation of the references to colour in this figure legend, the reader is referred to the Web version of this article.)

2.2. Chronology

The chronology of HS4 was established independently by U-Th dating and layer counting. Twenty-one subsamples were sampled and prepared in a class-1000 clean lab before being analyzed by multi-collector inductively coupled plasma mass spectrometry (MC-ICP-MS) at Oxford University (Nu Instruments), following the techniques of Robinson et al. (2002). Layer counting was used for the uppermost 150 years and U-Th dating for the period ca. 378 ± 57 to 9446 ± 146 years BP. The chronology of each sample is based on linear interpolation between the ^{230}Th dates, the average age uncertainty is 67 yrs. Further details on the chronological techniques and model were reported by Hu et al. (2008b).

2.3. pH measurement

The pH of cave surface sediments and overlying soils was measured following the methods of Yang et al. (2014). Samples were mixed with ultrapure water in a ratio of 1:2.5 (g/mL). After standing for 30 min, the pH of the supernatant was measured using a pH meter with a precision of ±0.01.

2.4. Lipid extraction and work-up

The stalagmite samples were treated with an optimized acid digestion method following Wang et al. (2012). In brief, 10 g of stalagmite sample were digested with 3 M HCl, then re-fluxed at 130 °C for 3 h with a condenser/heating mantle assembly. An internal standard (pregn-5-en-3.beta.-ol) was quantitatively added to each sample to quantify the amount of lipids in the stalagmite. After cooling, the residue was extracted by dichloromethane (15mL × 4) and the extracts combined. Solvents were removed by rotary evaporation (Buchi R210) under reduced pressure. Soil samples and cave surface sediments underwent the same work-up protocol as the stalagmite samples. The condensed lipids were further derivatized by BF_3-methanol (14% BF_3/methanol, Sigma) and BSTFA (N, O-bis(trimethylsilyl) trifluoroacetamide, Supelco) before undergoing gas chromatography-mass spectrometry (GC-MS). In order to minimize contamination, all glassware was soaked in a decontamination solution, rinsed with ultra purified water, and heated for 6 h at 500 °C. The HCl was pre-extracted with dichloromethane (DCM, × 4), and all other reagents were tested for background contaminants.

2.5. Instrumental analysis

All the samples were analyzed using GC-MS with a Hewlett Packard 6890 gas chromatograph coupled to a Hewlett Packard 5973 mass selective detector. Separation was performed on a ZB-5MS fused silica capillary column (60 m × 0.25 mm id.; 0.25 μm

film thickness). The GC oven temperature was programmed from 70 °C to 200 °C at 10 °C per min, then from 200 °C to 300 °C at 2 °C per min, and finally held at 300 °C for 27 min. The carrier gas was He (1 mL/min). The spectrometers were operated in electron-impact (EI) mode, the ionization energy was set at 70 eV and the scan range was from 50 to 550 aum.

2.6. Proxy calculation

The RAN_{15} and RIAN in the HS4 stalagmite samples were calculated using the relative abundances of the 3-OH-FAs with carbon numbers from C_{10} to C_{18}, which are derived from Gram-negative bacteria. Standard deviations for the RAN_{15}-MAAT and RIAN were calculated by a duplicate extraction and analyses on 9 randomly selected samples.

3. Results and discussion

3.1. Distribution and source of 3-OH-FAs

Below we discuss the distributional characteristics of 3-OH-FAs in Heshang Cave sediments and overlying soils and, with consideration of recent bacterial monitoring of the cave environment and drip waters (Liu et al., 2010; Yun et al., 2016b), constrain their possible sources and pathways.

The average distributions of 3-OH-FAs in the overlying soils, cave surface sediments and the HS4 stalagmite samples are illustrated in Fig. 2. There is an overall similarity in the distribution patterns of the three sample sets (with some differences discussed below), with the *n*-C_{10}, *n*-C_{12}, *n*-C_{14}, *n*-C_{16} and *n*-C_{18} homologues being typically most abundant. The carbon number of the detectable 3-OH-FA homologues varies from C_8 to C_{30} (Fig. 2). However, only the overlying soil samples contain the lowest carbon numbers of the 3-OH-FAs (*n*-C_8, *i*-C_9, *n*-C_9) (Fig. 2A). The distribution of 3-OH-FAs in the HS4 stalagmite reported here agrees with previous studies of the HS4 stalagmite from Heshang Cave (Huang et al., 2008; Wang et al., 2012). The only other reports of 3-OH-FAs in speleothem samples comes from an Ethiopian stalagmite (Blyth et al., 2006) and a British stalagmite (Blyth et al., 2011). The molecular distributions reported by Blyth et al. (2006) and (2011) are similar (maxima at *n*-C_{12}, *n*-C_{14}, *n*-C_{16} etc.) to the HS4 distributions, but the higher molecular weight 3-OH-FAs (>C_{20}) we detected were not previously reported.

Normal and branched 3-OH-FAs homologues of C_{10} to C_{18} chain length are abundant constituents of Lipid A, a constituent of LPS, the main component of the outer membrane of Gram-negative bacteria (Lee et al., 2004; Szponar et al., 2003). 3-OH-FAs have been used to quantify and characterize the Gram-negative bacterial community in atmospheric aerosols (Lee et al., 2004), marine dissolved organic matter (DOM) (Wakeham et al., 2003) and snow samples (Tyagi et al., 2015, 2016), and have recently been utilized to define a number of novel terrestrial paleoclimate proxies (Wang et al., 2016). The fractional abundance of the individual 3-OH-FA homologues varies from 0 to 30% in the studied samples. The 3-OH-FAs generally show a strong even/odd predominance (Fig. 2). In the HS4 stalagmite, this general even/odd predominance is accentuated for the homologues in the range from C_{11} to C_{15}, but is reversed for the *i*-C_{17} 3-OH-FA which is notably higher than the *n*-C_{16} 3-OH-FA (Fig. 2C). Furthermore, the *n*-C_{12} 3-OH-FA accounts for ca.18% in the stalagmite samples, but only ca.11% in both the overlying soils and cave surface sediments. The higher proportion of *n*-C_{12} and *i*-C_{17} homologues in the stalagmite may derive from *in situ* bacterial production or possibly better preservation of these compounds in stalagmites.

Culturable bacteria in drip waters from Heshang Cave are dominated by Gram-negative heterotrophs, derived from Proteobacteria with the dominance of Gamma proteobacteria (Liu et al., 2010). A two-year drip water monitoring experiment in Heshang

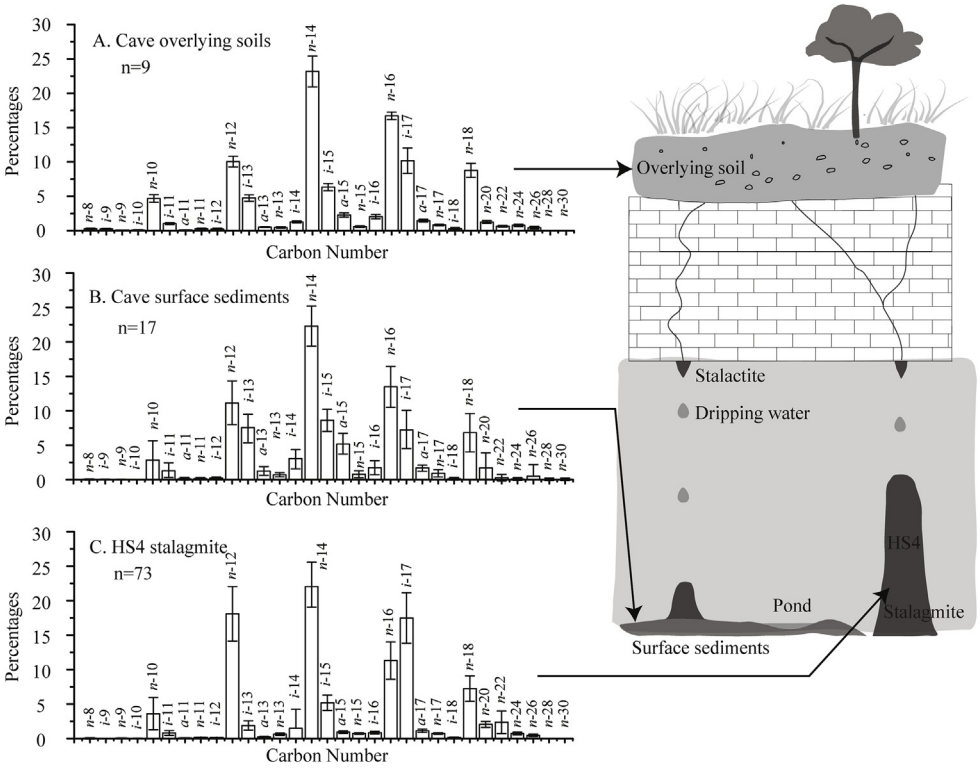

Fig. 2. Distribution and fractional abundance of 3-hydroxy fatty acid homologues in (A) cave overlying soils, (B) cave surface sediments, and (C) HS4 stalagmite samples.

Cave likely demonstrates a pathway for transporting 3-OH-FAs from the overlying soil microbial community to cave sediments and speleothem surfaces (Li et al., 2011). Meanwhile, a recent molecular survey of bacterial communities in Heshang Cave drip waters, over the period of 2008–2013, confirms a diverse Gram-negative bacterial community and reveals a seasonal control on Proteobacteria, whereby Beta-proteobacteria are supplied in the summer and Gamma-proteobacteria in the winter (Yun et al., 2016b). A latest investigation shows that Proteobacteria are both abundant in Heshang Cave overlying soils and drip waters (Yun et al., 2016a). This demonstrates that the seasonal signal of changes in the Gram-negative bacterial community is transmitted readily through the Heshang Cave system to drip waters and to the cave and speleothems. This seasonal cycle is positive from a paleoclimate perspective, suggesting minimal attenuation of bacterial based climate signals transmitted from the overlying soils to the HS4 stalagmite, at least sufficient for centennial to millennial scale paleoclimate studies.

As noted above, a distinctive feature of the 3-OH-FA distribution in the HS4 samples, is the greater relative abundance of the *n*-C_{12} and *i*-C_{17} 3-OH-FAs compared to both overlying soils and cave surface sediments (Fig. 2). This may suggest an additional contribution of 3-OH-FAs, derived from microbes from the cave drip water, which are sequestered and trapped in the calcite matrix (Supplementary Information). We note that Pacton et al. (2013) report that microbial activity can initiate calcite deposition in the aphotic zone of caves before inorganic precipitation of carbonates. We also note the low abundances of long chain 3-OH-FAs (C_{20}-C_{26}), which might originate from fungi, and/or Gram-positive actinomycetes (Keinänen et al., 2003). However, we suggest that the broad similarity of 3-OH-FA distributions in the overlying soils and stalagmites, supported by the site-specific analyses of bacterial diversity and transport pathways (Liu et al., 2010; Yun et al., 2016b), supports a major contribution of 3-OH-FAs from Gram-negative bacteria dwelling in the overlying soils to the HS4 stalagmite samples. This is consistent with previous findings that lipids preserved in speleothems are principally derived from the overlying soil ecosystem and vegetation, having been transported from the surface by percolating groundwater, although a proportion may be derived from the cave ecosystem (Blyth et al., 2014; Xie et al., 2003, 2005; Yang et al., 2011).

3.2. Holocene hydrological reconstruction

Recent work has demonstrated that pH is a key environmental parameter in controlling soil bacterial community structure and diversity (Bååth and Anderson, 2003; Griffiths et al., 2011; Lauber et al., 2009; Shen et al., 2013; Zhang et al., 2015). Notably, Giotis et al. (2007) found that a strain of Gram-negative bacterium increased/decreased the proportion of branched-chain fatty acids in higher pH/lower pH conditions. Recently, a novel pH proxy RIAN which is based on Gram-negative bacterial derived 3-OH-FAs in soils from Shennongjia Mountain was proposed by Wang et al. (2016), with a low RIAN value when pH is high. Based on our finding that 3-OH-FAs in the HS4 stalagmite are mainly derived from the overlying soils, here we interpret the HS4 RIAN record as reflecting local changes of pH (Fig. 3A). We note that the HS4 RIAN record is, for the period of mutual overlap, consistent with hydrological records based on hopanoids from the Dajiuhu peatland (Xie et al., 2013) (Fig. 3B; Supplementary Information), situated 130 km to the NW of Heshang Cave and the proportion of soil-derived magnetic minerals ($IRM_{soft\text{-}flux}$) incorporated into the HS4 stalagmite, which Zhu et al. (2017) interpret as a proxy for rainfall amount and intensity, with sensitivity to extreme precipitation events (Fig. 3C). These consistent lines of evidence demonstrate RIAN could be used as qualitative hydrological proxy in stalagmites. We argue below that, for the HS4 record, when effective precipitation was higher in the past, the RIAN value is lower and likely indicates enhanced leaching of soils and the influence of higher groundwater pH on the 3-OH-FA producing Gram-negative bacteria.

In soil environments, pH reflects the balance between precipitation and evaporation (e.g. hydrologically effective precipitation) and water movement through the soil. Rainwater is naturally acidic due to the reaction with CO_2 in the atmosphere to form carbonic acid. Excess rainfall leaches base cations increasing the relative percentage of H^+ and Al^{3+} ions (and thus acidity) in water. Soil temperatures, pH and aeration conditions also affect soil microbial activity and diversity which determines bacterial respiration of CO_2 (and the formation of carbonic acid), further influencing the pH of soil water and the degree of leaching (Fairchild and Baker, 2012). Thus we argue that in the soils above Heshang Cave, during the Holocene, pH was lower with higher effective precipitation (and vice versa). This is consistent with the generally observed relationship between effective precipitation and pH in global soils (Slessarev et al., 2016; Yang et al., 2014) and wider evidence of the substantial influence of pH on bacterial communities at both local and continental scales (Lauber et al., 2009; Rousk et al., 2010). However, on the contrary, changes of pH in groundwater systems may display in an opposite trend to that of the overlying soils in response to increased effective precipitation. In a well-drained karst landscape, increases in precipitation will also be associated with the increased movement of material (including organic matter and biomarkers), in dissolved or colloidal form to the groundwater system, which may ultimately percolate or flush into cave systems (Blyth et al., 2008). The pH of the groundwater is greatly affected by soil-derived colloids and fine sands flushed into the groundwater system (Fairchild and Baker, 2012). The soil processes outlined above influence the latter source of material and thus contribute to the pH of the groundwater system. More importantly, increased rainfall can result in a fall in the total cation content which will lead to an increase of pH in the groundwater system (Fairchild and Baker, 2012). Thus increased effective precipitation may lead to antiphased pH variations between the overlying soils and underlying groundwater systems. Here we interpret Holocene changes in RIAN in the HS4 stalagmite record as primarily reflecting local changes in precipitation regime which control the pH of the soil and groundwater systems. Specifically, we suggest that RIAN records increases in groundwater pH in response to increased rainfall, whereby microbes either initially derived from the overlying soils or already present in the groundwater system modified their membrane lipids to adapt to higher pH in the groundwater system resulting from increased rainfall and soil leaching.

From the above, hydrological changes during the last 9 ka BP were qualitatively reconstructed from the HS4 stalagmite using the RIAN proxy (Fig. 3), which we interpret as reflecting local changes in pH of the groundwater, originally driven by changes in precipitation. The RIAN record from HS4 reveals two (relatively long) wetter periods in central China, between 8.8 and 5.9 ka BP and 3.0–0 ka BP and one relatively dryer period from 5.9 to 3.0 ka BP (Fig. 3A). Both the HS4 and the Dajiuhu peatland records reconstruct a dry middle Holocene with decreased precipitation centered on ca. 5.5, 4.8 and 3.5 ka BP in central China (Fig. 3B and C) and overlap for two long wet periods between >9 ka to 6 ka BP and 3 to 0.6 ka BP. These drying events occur simultaneously with colder RAN_{15}-MAATs and heavier $\delta^{18}O$ values in HS4 (Fig. 4) and coeval cold/dry events recognized in a number of global Northern Hemisphere (NH) and regional paleoclimate records (Liu et al., 2013; Ljungqvist, 2010; Mayewski et al., 2004; Owen et al., 2016; Rohling and Palike, 2005). These proxy-inferred hydrological reconstructions re-enforce the conclusion of Xie et al. (2013) that the overturn of distinctive cultures in the Neolithic Period to Iron Age in

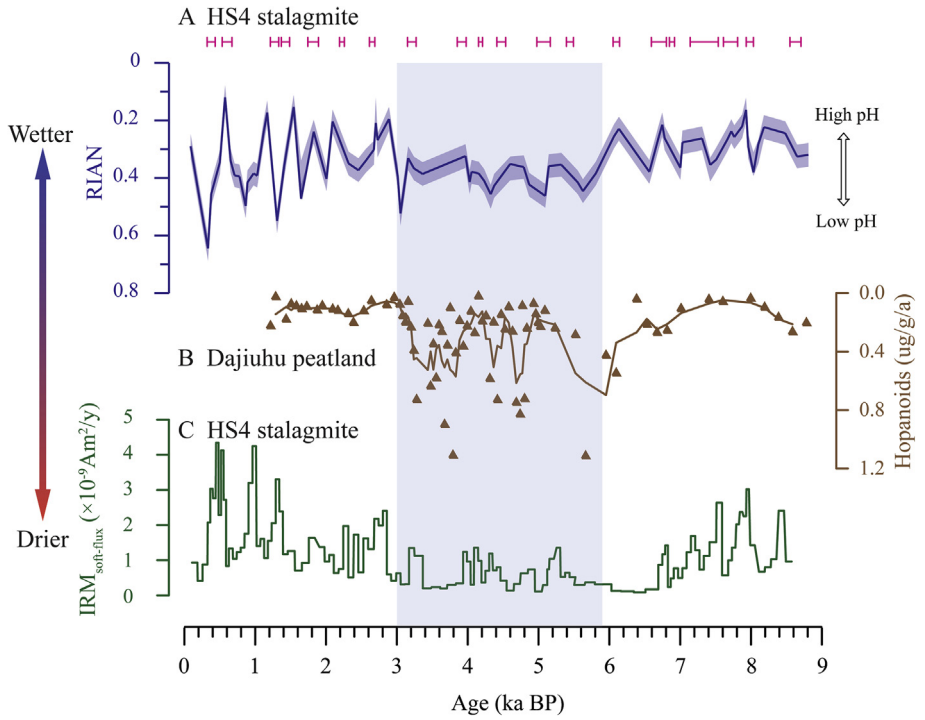

Fig. 3. Comparison of the HS4 RIAN record with other local and regional paleo-hydrological records. A) Heshang Cave hydrological record inferred from the RIAN record during the last 9 ka BP. U–Th dating errors (Hu et al., 2008b) are shown on the top of the RIAN curve as red line segments. B) Hydrological record based on hopanoids biomarkers from the Dajiuhu peatland (Xie et al., 2013), raw data are shown as triangle symbols, the black line is a locally weighted scatter plot smoothing with a quadratic polynomial (lowess) using a span of 5%. C) $IRM_{soft\text{-}flux}$ in stalagmite HS4. Peaks in $IRM_{soft\text{-}flux}$ indicate intervals with increased precipitation events (Zhu et al., 2017). (For interpretation of the references to colour in this figure legend, the reader is referred to the Web version of this article.)

central China (as observed in the distributions of >1600 prehistoric settlement sites) correlates with wet or flood episodes.

3.3. Holocene temperature reconstruction

Temperature changes during the last 9 ka BP were reconstructed from the HS4 stalagmite using the RAN_{15} proxy (Wang et al., 2016). RAN_{15} is a novel temperature proxy based on 3-OH-FA distributions measured in the soils from an altitudinal transect on Shennongjia Mountain located 120 km to the NW of Heshang Cave (Wang et al., 2016). Higher/lower RAN_{15} values (higher/lower ratio of the *anteiso* to *normal* C_{15} 3-OH-FAs) are obtained in soils with cooler/warmer MAATs. The quantitative correlation between MAAT and RAN_{15} is expressed in the following equation (Wang et al., 2016):

$$MAAT = 23.03 - 3.03 \times RAN_{15} \ (R^2 = 0.51,\ p < 0.001,\ RMSE = 2.6\ ^\circ C) \quad (1)$$

RAN_{15} in the HS4 stalagmite varies from 0.79 to 2.14 during the last 9 ka BP, with the lowest value at ca. 7.4 ka BP and highest value at ca. 0.5 ka BP (Fig. 4A). By applying equation (1) to the HS4 samples, we obtain RAN_{15}-MAAT reconstructions over the last 9 ka BP (Fig. 4A). The average RAN_{15}-MAAT of 18.4 °C over the most recent part of the record (<0.8 ka BP) overlaps with the range of MAATs, ca. 16.2 to 18.7 (av. 17.5 °C) measured since 1952 at the nearest meteorological station (Yichang, located ca. 100 km away) and is very close to the av. MAAT of 18 °C measured directly outside the cave by a temperature logger between 2004 and 2007 (Hu et al., 2008a). This agreement between reconstructed temperatures and instrumental measurements increases our confidence in the potential of the RAN_{15} proxy. RAN_{15}-MAATs in HS4 vary from 16.5 to 20.6 °C (av. 19 °C), during the last 9 ka BP, and broadly follow a long-term trend of declining temperatures in line with declining solar insolation at 30°N in July (Laskar et al., 2004) (Fig. 4B). The temperature variation (4.1 °C) in our record is larger than the calibration error of the RAN_{15} proxy (RMSE = 2.6 °C; Wang et al., 2016). The Holocene Climate Optimum (HCO) shown in the RAN_{15}-MAAT record is from 8 to 6 ka BP, with the highest temperature at ca. 7.0 ka BP (Fig. 4A). Superimposed on the orbital-scale Holocene trend are centennial to millennial scale climate fluctuations of ca. 1–2 °C (Fig. 4A). Interestingly, the most recent 0.9 ka BP is distinguished by greater variability with the highest (20.5 °C) and lowest (16.5 °C) RAN_{15}-MAATs occurring consecutively at 0.6 ka BP and 0.5 ka BP.

Our reconstructed RAN_{15}-MAAT follows a similar trend to the $\delta^{18}O$ record (Hu et al., 2008b) from the HS4 stalagmite (Fig. 4C). The high resolution HS4 $\delta^{18}O$ record encodes a mixture of temperature and hydrological signals and clearly defines a series of centennial scale episodes of heavier $\delta^{18}O$ (dry/cool events) superimposed on the longer term Holocene trend (Hu et al., 2008b). Although the novel biomarker based proxy has a relatively low resolution, it's worth noting that a number of cooler episodes observed in the HS4 RAN_{15}-MAAT record, centered on ca. 8.2 ka, 3.4 ka and 0.5 ka BP (little ice age, LIA) occur simultaneously with heavier values in the high resolution $\delta^{18}O$ record in HS4. Coeval cooling events are broadly recognized in a number of global NH and regional (monsoonal) paleoclimate records (Ljungqvist, 2010; Mayewski et al., 2004; Rohling and Palike, 2005). Notably our RAN_{15}-MAAT record is consistent with globally distal $\delta^{18}O$ ice-core record from Greenland (Johnsen et al., 2001) (Fig. 4D) and the Northern Hemisphere Holocene stacked temperature anomalies record (30°–90°N) (Marcott et al., 2013) (Fig. 4E). Although our sampling resolution is necessarily low due to biomarker sampling requirements (at this stage of analytical development), the HS4 age model is well constrained and we note that these RAN_{15}-MAAT

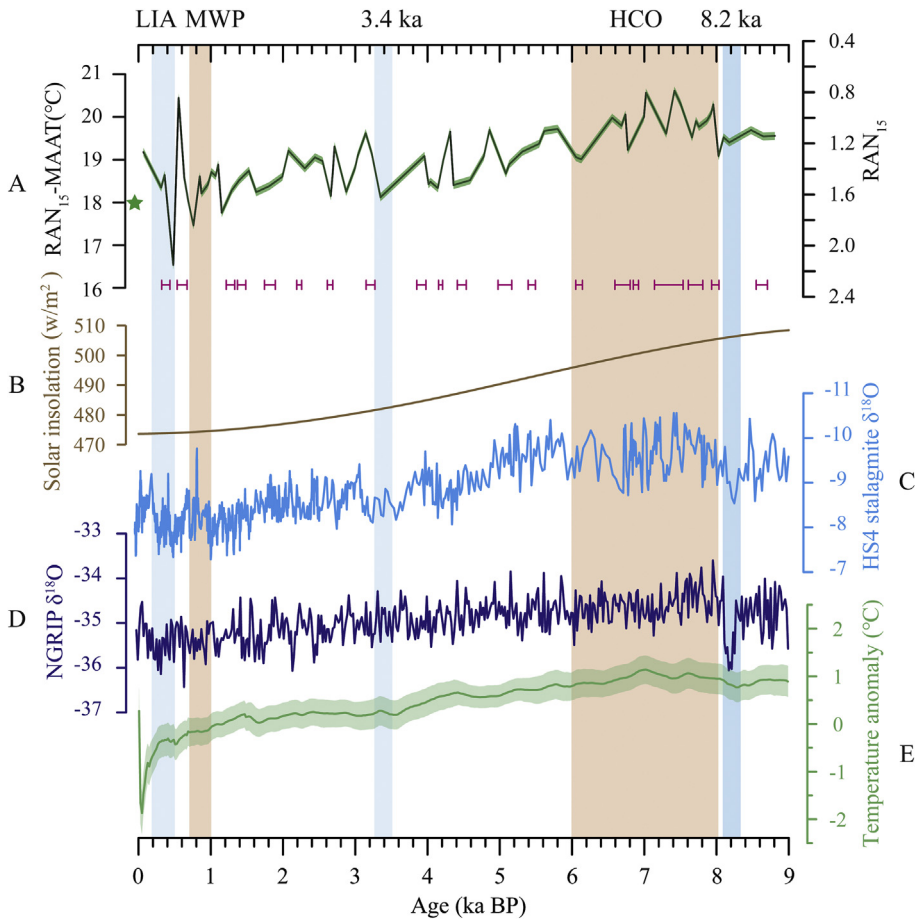

Fig. 4. Comparison of the HS4 stalagmite RAN_{15}-MAAT record with other time-series and proxy records. A) RAN_{15} and RAN_{15}-MAAT record reconstructed from the HS4 stalagmite. The standard deviation of the RAN_{15}-MAAT record is ±0.1 °C. The green star represents the mean annual air temperature (MAAT) immediately outside the cave, as by a temperature logger between 2004 and 2007 (Hu et al., 2008a). U–Th dating errors (Hu et al., 2008b) are shown on the bottom of the RAN_{15}-MAAT curve as red line segments. B) Solar insolation changes at 30°N in July during the last 9 ka BP (Laskar et al., 2004). C) The $CaCO_3$ oxygen isotope record from the HS4 stalagmite (Hu et al., 2008b). D) Ice core $\delta^{18}O$ record from North GRIP (Johnsen et al., 2001). E) The Northern Hemisphere stacked temperature anomalies (30°–90°N) for the 5° × 5° area-weighted mean calculation with its 1σ uncertainty (Marcott et al., 2013). (For interpretation of the references to colour in this figure legend, the reader is referred to the Web version of this article.)

maxima and minima at 0.6 ka BP and 0.5 ka BP coincide with NH scale warm and cold episodes during the late medieval warm periods (MWP) and LIA respectively (Ljungqvist, 2010; Mann et al., 2008; Moberg et al., 2005).

4. Conclusion

Hydrological and temperature changes in the middle reaches of the Yangtze River during the last 9 ka BP were reconstructed using Gram-negative membrane lipids extracted from the HS4 stalagmite from Heshang Cave, central China. RAN_{15} is a temperature proxy while RIAN is interpreted as a qualitative hydrological proxy. Temperatures varied from 16.5 to 20.6 °C during the last 9 ka BP, with a relatively warm period in the early to middle Holocene (8.0–6.0 ka BP), and then a relatively cool period in the late Holocene. The hydrological record shows two relatively long wet periods and one relatively dry period in central China, 8.8–5.9 ka BP, 3.0–0 ka BP and 5.9–3.0 ka BP respectively. The HS4 Holocene Climatic Optimum (HCO) between 8.0 and 6.0 ka BP is warmer and wetter than any other period in the Holocene and supports a conclusion of the seminal review of monsoon paleoclimate by An et al. (2000) that an early Holocene Optimum in monsoon strength occurred in the middle and lower reaches of the Yangtze River, China, centered on ca. 6 ka BP. Moreover, this agrees with an ensemble of 18 different model simulations (Joussaume et al., 1999) for 6 ka, which all indicate enhanced low-level convergence into the monsoon low over Eurasia, with the summer monsoon flow extending further inland. The present study demonstrates both the first paleoclimate application of 3-OH-FA based proxies and how such biomarker tools can record independent hydrological and temperature signals in speleothems.

Acknowledgements

Thanks to Prof. Ian Fairchild at University of Birmingham and Prof. Chaoyong Hu at China University of Geosciences for their valuable help on the manuscript and to Dr. Xuan Qiu at China University of Geosciences for his help during the bacterial culture experiment. This work was supported by the National Natural Science Foundation of China (grant nos. 41330103, 41773135, 41573099), the Key R&D Project of Ministry of Science and Technology (grant no. 2016YFA0601100), the 111 project (National Bureau of Foreign Experts and the Ministry of Education of China; grant no. B08030), and the Fundamental Research Funds for National University, China University of Geosciences Wuhan (grant no. CUGL170815). We thank the China Scholarship Council (CSC) (grant no. 201306410031) for supporting Canfa Wang's studies at the University of Birmingham.

References

An, Z., 2000. The history and variability of the East Asian paleomonsoon climate. Quat. Sci. Rev. 19, 171–187.

An, Z., Porter, S.C., Kutzbach, J.E., Xihao, W., Wang, S., Liu, X., Li, X., Zhou, W., 2000. Asynchronous Holocene optimum of the East Asian monsoon. Quat. Sci. Rev. 19, 743–762.

Bååth, E., Anderson, T.H., 2003. Comparison of soil fungal/bacterial ratios in a pH gradient using physiological and PLFA-based techniques. Soil Biol. Biochem. 35, 955–963.

Baker, A., Jex, C.N., Rutlidge, H., Woltering, M., Blyth, A.J., Andersen, M.S., Cuthbert, M.O., Marjo, C.E., Markowska, M., Rau, G.C., Khan, S.J., 2016. An irrigation experiment to compare soil, water and speleothem tetraether membrane lipid distributions. Org. Geochem. 94, 12–20.

Blyth, A.J., Asrat, A., Baker, A., Gulliver, P., Leng, M.J., Genty, D., 2007. A new approach to detecting vegetation and land-use change using high-resolution lipid biomarker records in stalagmites. Quat. Res. 68, 314–324.

Blyth, A.J., Baker, A., Collins, M.J., Penkman, K.E.H., Gilmour, M.A., Moss, J.S., Genty, D., Drysdale, R.N., 2008. Molecular organic matter in speleothems and its potential as an environmental proxy. Quat. Sci. Rev. 27, 905–921.

Blyth, A.J., Baker, A., Thomas, L.E., Van Calsteren, P., 2011. A 2000-year lipid biomarker record preserved in a stalagmite from north-west Scotland. J. Quat. Sci. 26, 326–334.

Blyth, A.J., Farrimond, P., Jones, M., 2006. An optimised method for the extraction and analysis of lipid biomarkers from stalagmites. Org. Geochem. 37, 882–890.

Blyth, A.J., Hartland, A., Baker, A., 2016. Organic proxies in speleothems – new developments, advantages and limitations. Quat. Sci. Rev. 149, 1–17.

Blyth, A.J., Jex, C.N., Baker, A., Khan, S.J., Schouten, S., 2014. Contrasting distributions of glycerol dialkyl glycerol tetraethers (GDGTs) in speleothems and associated soils. Org. Geochem. 69, 1–10.

Blyth, A.J., Schouten, S., 2013. Calibrating the glycerol dialkyl glycerol tetraether temperature signal in speleothems. Geochem. Cosmochim. Acta 109, 312–328.

Blyth, A.J., Watson, J.S., Woodhead, J., Hellstrom, J., 2010. Organic compounds preserved in a 2.9 million year old stalagmite from the Nullarbor Plain, Australia. Chem. Geol. 279, 101–105.

Bosle, J.M., Mischel, S.A., Schulze, A.L., Scholz, D., Hoffmann, T., 2014. Quantification of low molecular weight fatty acids in cave drip water and speleothems using HPLC-ESI-IT/MS—development and validation of a selective method. Anal. Bioanal. Chem. 406, 3167–3177.

Castañeda, I.S., Schouten, S., 2011. A review of molecular organic proxies for examining modern and ancient lacustrine environments. Quat. Sci. Rev. 30, 2851–2891.

Dreybrodt, W., Scholz, D., 2011. Climatic dependence of stable carbon and oxygen isotope signals recorded in speleothems: from soil water to speleothem calcite. Geochem. Cosmochim. Acta 75, 734–752.

Eglinton, T., Eglinton, G., 2008. Molecular proxies for paleoclimatology. Earth Planet Sci. Lett. 275, 1–16.

Fairchild, I., Smith, C., Baker, A., Fuller, L., Spötl, C., Mattey, D., McDermott, F., 2006. Modification and preservation of environmental signals in speleothems. Earth Sci. Rev. 75, 105–153.

Fairchild, I.J., Baker, A., 2012. Speleothem Science: from Process to Past Environments. Wiley, Chichester.

Giotis, E.S., McDowell, D.A., Blair, I.S., Wilkinson, B.J., 2007. Role of branched-chain fatty acids in pH stress tolerance in *Listeria monocytogenes*. Appl. Environ. Microbiol. 73, 997–1001.

Gong, L., Wang, H., Xiang, X., Qiu, X., Liu, Q., Wang, R., Zhao, R., Wang, C., 2015. pH shaping the composition of *sqhC*-containing bacterial communities. Geomicrobiol. J. 32, 433–444.

Griffiths, R.I., Thomson, B.C., James, P., Bell, T., Bailey, M., Whiteley, A.S., 2011. The bacterial biogeography of British soils. Environ. Microbiol. 13, 1642–1654.

Hu, C., Henderson, G., Huang, J., Chen, Z., Johnson, K., 2008a. Report of a three-year monitoring programme at Heshang Cave, Central China. Int. J. Speleol. 37, 143–151.

Hu, C., Henderson, G.M., Huang, J., Xie, S., Sun, Y., Johnson, K.R., 2008b. Quantification of Holocene Asian monsoon rainfall from spatially separated cave records. Earth Planet Sci. Lett. 266, 221–232.

Huang, X., Cui, J., Pu, Y., Huang, J., Blyth, A.J., 2008. Identifying "free" and "bound" lipid fractions in stalagmite samples: an example from Heshang Cave, Southern China. Appl. Geochem. 23, 2589–2595.

Huguet, C., Routh, J., Fietz, S., Lone, M.A., Kalpana, M., Ghosh, P., Mangini, A., Kumar, V., Rangarajan, R., 2018. Temperature and monsoon tango in a tropical stalagmite: last glacial-interglacial climate dynamics. Sci. Rep. 8, 5386.

IPCC, 2014. Summary for policymakers. In: Field, C.B., Barros, V.R., Dokken, D.J., Mach, K.J., Mastrandrea, M.D., Bilir, T.E., Chatterjee, M., Ebi, K.L., Estrada, Y.O., Genova, R.C., Girma, B., Kissel, E.S., Levy, A.N., MacCracken, S., Mastrandrea, P.R., White, L.L. (Eds.), Climate Change 2014: Impacts, Adaptation, and Vulnerability. Part a: Global and Sectoral Aspects. Contribution of Working Group II to the Fifth Assessment Report of the Intergovernmental Panel on Climate Change. Cambridge University Press, Cambridge, United Kingdom, and New York, NY, USA, pp. 1–32.

Johnsen, S.J., Dahl-Jensen, D., Gundestrup, N., Steffensen, J.P., Clausen, H.B., Miller, H., Masson-Delmotte, V., Sveinbjörnsdottir, A.E., White, J., 2001. Oxygen isotope and palaeotemperature records from six Greenland ice-core stations: Camp Century, Dye-3, GRIP, GISP2, Renland and NorthGRIP. J. Quat. Sci. 16, 299–307.

Johnson, K., Hu, C., Belshaw, N., Henderson, G., 2006. Seasonal trace-element and stable-isotope variations in a Chinese speleothem: the potential for high-resolution paleomonsoon reconstruction. Earth Planet Sci. Lett. 244, 394–407.

Joussaume, S., Taylor, K., Braconnot, P., Mitchell, J., Kutzbach, J., Harrison, S., Prentice, I., Broccoli, A., Abe-Ouchi, A., Bartlein, P., 1999. Monsoon changes for 6000 years ago: results of 18 simulations from the paleoclimate modeling intercomparison project (PMIP). Geophys. Res. Lett. 26, 859–862.

Keinänen, M.M., Korhonen, L.K., Martikainen, P.J., Vartiainen, T., Miettinen, I.T., Lehtola, M.J., Nenonen, K., Pajunen, H., Kontro, M.H., 2003. Gas chromatographic-mass spectrometric detection of 2- and 3-hydroxy fatty acids as methyl esters from soil, sediment and biofilm. J. Chromatogr. B 783, 443–451.

Lachniet, M.S., 2009. Climatic and environmental controls on speleothem oxygen-isotope values. Quat. Sci. Rev. 28, 412–432.

Laskar, J., Robutel, P., Joutel, F., Gastineau, M., Correia, A., Levrard, B., 2004. A long-term numerical solution for the insolation quantities of the Earth. Astron. Astrophys. 428, 261–285.

Lauber, C.L., Hamady, M., Knight, R., Fierer, N., 2009. Pyrosequencing-based assessment of soil pH as a predictor of soil bacterial community structure at the continental scale. Appl. Environ. Microbiol. 75, 5111–5120.

Lee, A.K.Y., Chan, C.K., Fang, M., Lau, A.P.S., 2004. The 3-hydroxy fatty acids as biomarkers for quantification and characterization of endotoxins and Gram-negative bacteria in atmospheric aerosols in Hong Kong. Atmos. Environ. 38, 6307–6317.

Li, X., Hu, C., Huang, J., Xie, S., Baker, A., 2014. A 9000-year carbon isotopic record of acid-soluble organic matter in a stalagmite from Heshang Cave, central China: paleoclimate implications. Chem. Geol. 388, 71–77.

Li, X., Wang, C., Huang, J., Hu, C., Xie, S., 2011. Seasonal variation of fatty acids from drip water in Heshang Cave, central China. Appl. Geochem. 26, 341–347.

Liu, Q., Wang, H., Zhao, R., Qiu, X., Gong, L., 2010. Bacteria isolated from dripping water in the oligotrophic Heshang cave in central China. J. Earth Sci. 21, 325–328.

Liu, Y.H., Henderson, G.M., Hu, C.Y., Mason, A.J., Charnley, N., Johnson, K.R., Xie, S.C., 2013. Links between the East Asian monsoon and north atlantic climate during the 8,200 year event. Nat. Geosci. 6, 117–120.

Ljungqvist, F.C., 2010. A new reconstruction of temperature variability in the extra-tropical Northern Hemisphere during the last two millennia. Geografiska Annaler:Series A 92, 339–351.

Mann, M.E., Zhang, Z., Hughes, M.K., Bradley, R.S., Miller, S.K., Rutherford, S., Ni, F., 2008. Proxy-based reconstructions of hemispheric and global surface temperature variations over the past two millennia. In: Proceedings of the National Academy of Sciences, 105, pp. 13252–13257.

Marcott, S.A., Shakun, J.D., Clark, P.U., Mix, A.C., 2013. A reconstruction of regional and global temperature for the past 11,300 years. Science 339, 1198–1201.

Mayewski, P., Rohling, E., Curt Stager, J., Karlén, W., Maasch, K., David Meeker, L., Meyerson, E., Gasse, F., van Kreveld, S., Holmgren, K., 2004. Holocene climate variability. Quat. Res. 62, 243–255.

McDermott, F., 2004. Palaeo-climate reconstruction from stable isotope variations in speleothems: a review. Quat. Sci. Rev. 23, 901–918.

Moberg, A., Sonechkin, D.M., Holmgren, K., Datsenko, N.M., Karlén, W., 2005. Highly variable Northern Hemisphere temperatures reconstructed from low-and high-resolution proxy data. Nature 433, 613–617.

Owen, R.A., Day, C.C., Hu, C.Y., Liu, Y.H., Pointing, M.D., Blättler, C.L., Henderson, G.M., 2016. Calcium isotopes in caves as a proxy for aridity: modern calibration and application to the 8.2 kyr event. Earth Planet Sci. Lett. 443, 129–138.

Pacton, M., Breitenbach, S.F.M., Lechleitner, F.A., Vaks, A., Rollion-Bard, C., Gutareva, O.S., Osintcev, A.V., Vasconcelos, C., 2013. The role of microorganisms in the formation of a stalactite in Botovskaya Cave, Siberia – paleoenvironmental implications. Biogeosciences 10, 6115–6130.

Robinson, L.F., Henderson, G.M., Slowey, N.C., 2002. U–Th dating of marine isotope stage 7 in Bahamas slope sediments. Earth Planet Sci. Lett. 196, 175–187.

Rohling, E.J., Palike, H., 2005. Centennial-scale climate cooling with a sudden cold event around 8,200 years ago. Nature 434, 975–979.

Rousk, J., Bååth, E., Brookes, P.C., Lauber, C.L., Lozupone, C., Caporaso, J.G., Knight, R., Fierer, N., 2010. Soil bacterial and fungal communities across a pH gradient in an arable soil. ISME J. 4, 1340–1351.

Schouten, S., Hopmans, E.C., Sinninghe Damsté, J.S., 2013. The organic geochemistry of glycerol dialkyl glycerol tetraether lipids: a review. Org. Geochem. 54, 19–61.

Shen, C., Xiong, J., Zhang, H., Feng, Y., Lin, X., Li, X., Liang, W., Chu, H., 2013. Soil pH drives the spatial distribution of bacterial communities along elevation on Changbai Mountain. Soil Biol. Biochem. 57, 204–211.

Slessarev, E., Lin, Y., Bingham, N., Johnson, J., Dai, Y., Schimel, J., Chadwick, O., 2016. Water balance creates a threshold in soil pH at the global scale. Nature 540, 567–569.

Szponar, B., Krasnik, L., Hryniewiecki, T., Gamian, A., Larsson, L., 2003. Distribution of 3-hydroxy fatty acids in tissues after intraperitoneal injection of endotoxin. Clin. Chem. 49, 1149–1153.

Szponar, B., Norin, E., Midtvedt, T., Larsson, L., 2002. Limitations in the use of 3-hydroxy fatty acid analysis to determine endotoxin in mammalian samples. J. Microbiol. Meth. 50, 283–289.

Tyagi, P., Kawamura, K., Bikkina, S., Mochizuki, T., Aoki, K., 2016. Hydroxy fatty acids in snow pit samples from Mount Tateyama in central Japan: implications for atmospheric transport of microorganisms and plant waxes associated with Asian dust. J. Geophys. Res.: Atmosphere 121, 13641–13660.

Tyagi, P., Yamamoto, S., Kawamura, K., 2015. Hydroxy fatty acids in fresh snow

samples from northern Japan: long-range atmospheric transport of Gram-negative bacteria by Asian winter monsoon. Biogeosciences 12, 7071–7080.
Vaughan, M.J., Maier, R.M., Pryor, B.M., 2011. Fungal communities on speleothem surfaces in Kartchner Caverns, Arizona. USA. International Journal of Speleology 40, 8.
Wakeham, S.G., Pease, T.K., Benner, R., 2003. Hydroxy fatty acids in marine dissolved organic matter as indicators of bacterial membrane material. Org. Geochem. 34, 857–868.
Wang, C., Bendle, J., Yang, Y., Yang, H., Sun, H., Huang, J., Xie, S., 2016. Impacts of pH and temperature on soil bacterial 3-hydroxy fatty acids: development of novel terrestrial proxies. Org. Geochem. 94, 21–31.
Wang, C., Zhang, H., Huang, X., Huang, J., Xie, S., 2012. Optimization of acid digestion conditions on the extraction of fatty acids from stalagmites. Front. Earth Sci. 6, 109–114.
Webster, P.J., Magana, V.O., Palmer, T., Shukla, J., Tomas, R., Yanai, M., Yasunari, T., 1998. Monsoons: processes, predictability, and the prospects for prediction. J. Geophys. Res.: Oceans 103, 14451–14510.
Wollenweber, H.-W., Rietschel, E.T., 1990. Analysis of lipopolysaccharide (lipid A) fatty acids. J. Microbiol. Meth. 11, 195–211.
Wong, C.I., Breecker, D.O., 2015. Advancements in the use of speleothems as climate archives. Quat. Sci. Rev. 127, 1–18.
Xie, S., Evershed, R.P., Huang, X., Zhu, Z., Pancost, R.D., Meyers, P.A., Gong, L., Hu, C., Huang, J., Zhang, S., 2013. Concordant monsoon-driven postglacial hydrological changes in peat and stalagmite records and their impacts on prehistoric cultures in central China. Geology 41, 827–830.
Xie, S., Huang, J., Wang, H., Yi, Y., Hu, C., Cai, Y., Cheng, H., 2005. Distributions of fatty acids in a stalagmite related to paleoclimate change at Qingjiang in Hubei, southern China. Sci. China Earth Sci. 48, 1463–1469.
Xie, S., Yi, Y., Huang, J., Hu, C., Cai, Y., Collins, M., Baker, A., 2003. Lipid distribution in a subtropical southern China stalagmite as a record of soil ecosystem response to paleoclimate change. Quat. Res. 60, 340–347.
Yang, H., Ding, W., Zhang, C.L., Wu, X., Ma, X., He, G., Huang, J., Xie, S., 2011. Occurrence of tetraether lipids in stalagmites: implications for sources and GDGT-based proxies. Org. Geochem. 42, 108–115.
Yang, H., Pancost, R.D., Dang, X., Zhou, X., Evershed, R.P., Xiao, G., Tang, C., Gao, L., Guo, Z., Xie, S., 2014. Correlations between microbial tetraether lipids and environmental variables in Chinese soils: optimizing the paleo-reconstructions in semi-arid and arid regions. Geochem. Cosmochim. Acta 126, 49–69.
Yuan, D., Cheng, H., Edwards, R.L., Dykoski, C.A., Kelly, M.J., Zhang, M., Qing, J., Lin, Y., Wang, Y., Wu, J., Dorale, J.A., An, Z., Cai, Y., 2004. Timing, duration, and transitions of the last interglacial Asian monsoon. Science 304, 575–578.
Yun, Y., Wang, H., Man, B., Xiang, X., Zhou, J., Qiu, X., Duan, Y., Engel, A.S., 2016a. The relationship between pH and bacterial communities in a single karst ecosystem and its implication for soil acidification. Front. Microbiol. 7.
Yun, Y., Xiang, X., Wang, H., Man, B., Gong, L., Liu, Q., Dong, Q., Wang, R., 2016b. Five-year monitoring of bacterial communities in dripping water from the Heshang Cave in central China: implication for paleoclimate reconstruction and ecological functions. Geomicrobiol. J. 33, 553–563.
Zhang, Y., Cong, J., Lu, H., Li, G., Xue, Y., Deng, Y., Li, H., Zhou, J., Li, D., 2015. Soil bacterial diversity patterns and drivers along an elevational gradient on Shennongjia Mountain, China. Microb Biotechnol 8, 739–746.
Zhu, Z., Feinberg, J.M., Xie, S., Bourne, M.D., Huang, C., Hu, C., Cheng, H., 2017. Holocene ENSO-related cyclic storms recorded by magnetic minerals in speleothems of central China. Proc. Natl. Acad. Sci. U. S. A. 114, 852–857.